sciendo

POLISH MARITIME RESEARCH 4 (112) 2021 Vol. 28; pp. 30-41
10.2478/pomr-2021-0047

EVALUATION OF EFFECTIVENESS OF WATERJET PROPULSOR FOR A SMALL UNDERWATER VEHICLE

Lech Rowinski*
Gdańsk University of Technology, Poland
Maciej Kaczmarczyk

* Corresponding author: *rowinski@pg.edu.pl (L.Rowiński)*

ABSTRACT

The goal of the project described is to replace the existing propulsion system of a small underwater vehicle with a solution less prone to mechanical damage and ensuring a lower risk of the entanglement of fibrous objects suspended in the body of water. Four typical marine screws are utilised in the current design of the vehicle. One possible solution of the problem is the application of waterjet propulsors located inside the body of the vehicle instead. The general condition of the application of the new solution was to secure at least the same motion control capabilities of the vehicle while the basic capability is its propulsion effectiveness at the required speed. Specific features of the considered waterjet propulsor, when compared with their application in surface vessel propulsion, are the lack of the head losses and the low significance of cavitation issues. One of the difficulties in the considered case is the small diameter of the propulsor in comparison to commercially available waterjet units, which have diameters between 0.1 [m] and 1.0 [m]. There is very little data regarding the design and performance of devices in the 0.02 to 0.05 [m] range. Methods utilised to forecast the performance of the new propulsion system are presented and results compared. These were semi-empirical calculations, numerical calculations and tests of real devices. The algorithm that is based on semi-empirical calculations is of particular interest while it offers possibility quick assessment of performance of a propulsor composed of several well defined components. The results indicate the feasibility of modification of the propulsion system for the considered vehicle if all the existing circumstances are taken into account.

Keywords: ship propulsion, hydromechanics, waterjet, underwater vehicle

OVERALL CHARACTERISTICS OF THE GLUPTAK UNDERWATER VEHICLE

Small underwater vehicles offer the ultimate in autonomous remote subsea survey capability. These free-swimming autonomous underwater vehicles are characterised by great manoeuvrability and high accuracy of stabilisation. Due to their small size, operational efficiency and transport properties, the advantages of autonomous underwater vehicles outweigh the advantages of manned underwater vehicles. Their propulsion system is an important element in energy conversion to generate a reaction sequence that consists of thrust momentum and pressure thrust. One of the possible solutions to ensure the appropriate values of these parameters is the use of water jet propulsion system. Many different scientific and research centers are working on the solution of the effectiveness of this type of drive, the result of which can be found in many publications in this field, e.g. in [1], [2], [3] and [4].

In [1], an integrated magnetically slotless PM brushless machine having 2-segment Halbach array was proposed to employ in novel shaftless pump-jet propulsor the autonomous underwater vehicle. The optimal magnet ratio array was analytically determined and the electromagnetic performance of target machine is analysed by finite-element analysis. In order to exam the effectiveness of cooling system, a thermal and computational fluid dynamic coupled analysis was developed. The overall analysis results reveal that the

proposed magnetically slotless PM brushless machine achieves design requirements and capable for using in the units having shaftless pump-jet.

The performance parameters of waterjet propulsion, such as resistance, waterjet thrust, thrust deduction, and the physical quantity of the control volume, were solved by iteration and thy presented in [2]. Authors applied the proposed approach and the RANS CFD method to a waterjet propelled trimaran model. Although there were some differences between the two methods in terms of the local pressure distribution and thrust deduction, the relative error in the evaluation results for the waterjet propulsion performance was generally reasonable and acceptable. This indicates that the proposed method can be used at the early stages of ship design without partial information about the waterjet propulsion system, and especially in the absence of a physical model of the pump.

In [3] Authors present a numerical investigation into four different nozzles (cos, exponent, cylindrical and conical ones) for the water jet propulsion system of underwater vehicles. The effects of geometric parameters (length and wall roughness) and dynamic parameter (backpressure with constant pressure difference) of four different nozzles on the momentum thrust, average fluid velocity and vapour mass flow rate were analysed. The governing equations were solved through CFD software. The results showed that cos nozzle which produces more momentum thrust is the most appropriate, and the nozzle length L is proposed to set 36 mm. The effects of wall roughness were different on four nozzles, and the smooth inner wall was proposed for cos nozzles.

A special framework that allows you to determine the effectiveness of the water jet propulsion system is presented in [4]. This framework provided a basis for minimizing the waterjet propelled energy consumption through a proper force weighting.

The Gluptak underwater vehicle, as shown in the Fig. 1, was developed at Ship design department of Gdansk University of Technology [5], [6], [7]. It is a small, slow-moving, torpedo-like object. It is supplied with energy from an internal source (battery) and controlled remotely by means of an optical fibre. It is used to identify and destroy naval mines. The vehicle is able to flow at velocity of 3 [m/s] relative to the water. One of the limiting factors of the vehicle performance is the limited energy capacity of the internal battery pack and the power available for propulsion. Therefore, two basic parameters define the propulsion system. These are the available thrust and the widely understood overall efficiency. Additional factors are requirements regarding high manoeuvrability of the vehicle. In the horizontal plane, the vehicle is propelled by means of four screw propellers. The fifth propeller, built into the vehicle's hull, is used to control its vertical movement. It was placed at the centre of the vertical drag of the vehicle to ascend and descend at zero forward speed. The horizontal propellers are arranged in an X configuration as shown in the Fig. 3. Additionally, the axes of the propeller shafts are inclined 7 degrees relative to the longitudinal axis of the vehicle. Such an inclination angle is high enough to double the turning moment generated by the propellers with reference to the vertical axis of the vehicle.

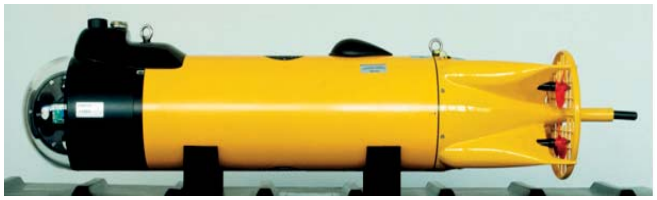

Fig. 1. Side view of the Gluptak vehicle. Length of the vehicle is 1.4 [m] and hull diameter is 0.25 [m]. Length of the stern, propulsion section is limited to 0.33 [m]

While the vehicle is moving forward, the left pair of propellers rotates anticlockwise and the right pair rotates clockwise. This solution helps to stabilise the vehicle and to reduce the rolling moment acting on the vehicle. This rolling moment is caused by torque of the propellers and changes of the speed of the motors due to inertia of the rotating components. To facilitate the manoeuvrability of the vehicle, the speed of each propeller is linearly controlled in the range of $\pm$3200 [rpm]. The highest sea current that allows for manoeuvring using turning moment is 0.5 [m/s]. The moment is generated by two pairs of horizontal propellers working in opposite directions. Above this velocity, the vehicle is only capable of moving forward, against the current. It can be inclined from the current line a few degrees in any direction by means of differentiating the speed of the propellers. In still, calm water, the Gluptak vehicle is able to manoeuvre quite well. However, reversing of the horizontal propellers is to be avoided due to the danger of mechanical destruction of the tether cable (the control fibre).

The screw propellers of the Gluptak vehicle are 0.1 [m] diameter, three-blade Wageningen B series propellers with a 0.3 surface coefficient and P/D=0.635. They are designed to operate with optimum performance (high thrust) in the forward direction. The propeller geometry was calculated using the typical procedure and corrected for real working conditions using experimental evaluation. The propeller's K_T, K_Q and η characteristics are presented in the Fig. 2.

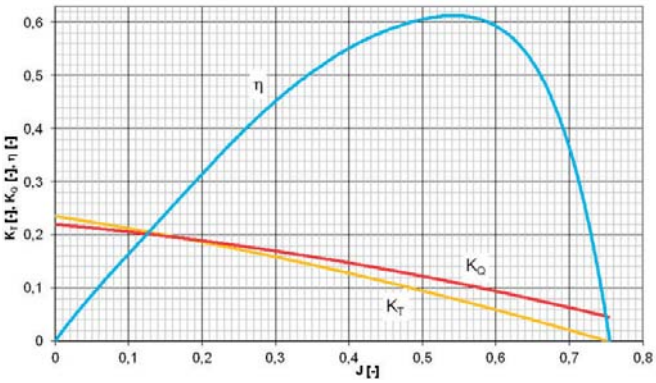

Fig. 2. The K_T and K_Q coefficient as well as η of the PG-100 propeller designed for a cruising speed of 3 [m/s] - three-blade Wageningen B series propellers have 0.3 surface coefficient and P/D=0.635

The propulsion system based on screw propellers proved to be effective in assumed conditions. However, the propellers are vulnerable to mechanical damage. They are in danger of sucking in quantities of different debris floating in the water (such as small stones, seaweed, ropes, tethers etc.). An example of such an incident is shown in the Fig. 3(a). The case presented indicates that comparatively thick (3 [mm] diameter) cable, reinforced with aramide fibre, can be easily sucked into the propeller and cause damage. The problem is obviously more serious in the case of the bare optical cable that is also utilised for vehicle control in the case of a combat mission. The optical fibre utilised for this purpose is only 0.25 [mm] thick and very fragile (made of glass). To reduce the risks and improve the handling capability, a grill guard was developed as the simplest solution to this problem. Its effectiveness has been proved during a series of experiments. The solution is not perfect but works to an acceptable extent. However, the introduction of the grill increases the drag force of the vehicle by approximately 35%. Such an increase of the drag is critically negative factor for the vehicle, which is supplied by an internal source of energy that offers limited power and capacity. Considering the grill guard to be a part of the propulsion system, the total efficiency of this system is approximately 40% and well below the 60% efficiency of the arrangement without the grill guard.

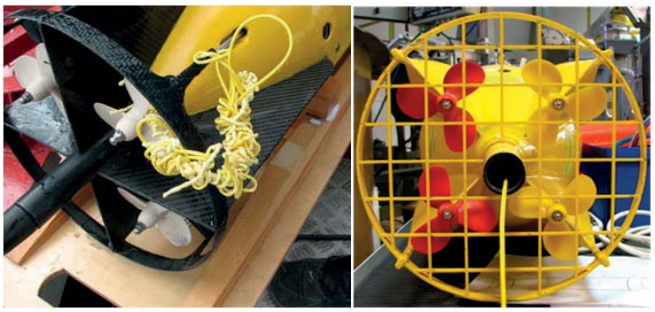

Fig. 3. Propeller of the Gluptak vehicle: a) the aramide reinforced tether cable entangled in one of the propellers of the Gluptak vehicle; b) arrangement of set of four screw propellers of the Gluptak vehicle, with the fibre protection grill guard (the directivity of the propellers is colour-coded to avoid mistakes during assembly)

DRAG FORCE OF THE GLUPTAK VEHICLE AND PROPULSOR DESIGN CONSTRAINTS

The external hull of the Gluptak vehicle is composed of the spherical bow, the cylindrical middle section and the conical stern section. The conical stern section contains propulsion components such as electric motors and propulsion shafts. Drag force curves of the Gluptak vehicle in different configurations that were investigated (measured) are shown in the Fig. 4. Differences between the bare hull and hulls with waterjet propulsors compared to the hull equipped with the grill guard are easily visible. To achieve a velocity of 3.0 [m/s], the vehicle body equipped with the grill guard requires 75 [N] of thrust. For the vehicle body without the grill and slightly deformed by the presence of waterjets, 50–56 [N] of thrust force is required. An outsourced CFD analysis for the vehicle with water jet drives (WJ39G, which stands for off-the-shelf Graupner's water jet propulsion with 39 [mm] of rotor diameter) suggested nearly 41 [N] of the drag and it was underestimated by over 12%. Typically, for underwater vehicles such simulations lower the results in range of 20-30%.

The vehicle drag force is not the only constraint in the design of the propulsion suite of the Gluptak vehicle. Its geometrical configuration is limited by the available length of the stern section of the vehicle. The diameter of the flow tunnel of the propulsor and therefore the diameter of its rotor need to be kept at the minimum to ensure smooth flow around the stern. There are also issues that are not directly important problems for unidirectional propulsion. While the fins and the protection grill of the current configuration provide the vehicle with directional stability, this function needs to be ensured by a new arrangement. The manoeuvre properties and spatial orientation (location) of the water intakes must also be considered. However, investigations regarding these issues are not described in this paper.

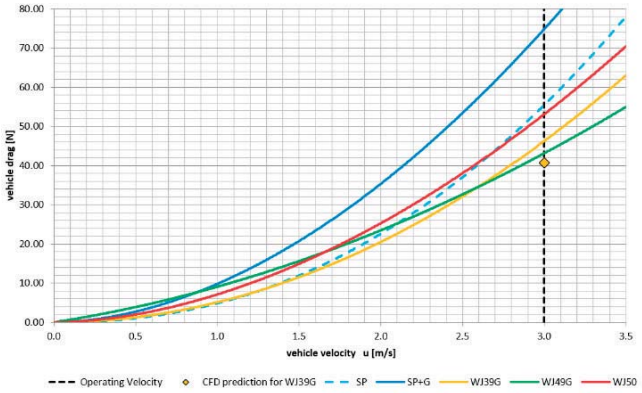

Fig. 4. Drag curves of the Gluptak vehicle in different configurations. SP – standard propellers, SP+G – standard propellers with protective grill, WJ39G – Graupner's water jet with 39 [mm] rotor diameter, WJ49G – Graupenr's water jet wit 49 [mm] rotor diameter, WJ50 – newly designed water jet with 50 [mm] rotor diameter

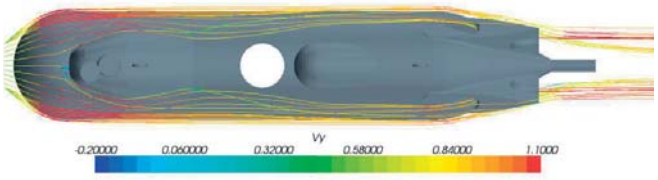

Fig. 5. Flow lines calculated for vehicle velocity of 3 [m/s] with pump rotors rotating (the colour scale: 1 -3 [m/s])

As a result of the analyses the following requirements and constraints were defined for the single propulsor design four-unit propulsion system:

thrust at vehicle velocity of 3 [m/s]:	=>14 [N]
diameter of the flow tunnel:	as small as feasible
total length of the propulsor:	<= 0.33 [m]
radial extension of the case of the propulsor outside the vehicle body:	<= 0.05 [m]
power requirement (at motor shaft)	<=120 [W]

The goal of the study was to evaluate the required propulsion power and total efficiency of the propulsor that meet the defined restrictions. To compare the overall performance of waterjet propulsors with different pump rotor diameters, a semi-empirical procedure was utilised. Particular phenomena were investigated using programmes that implement CFD methods. Finally, real experiments were run to verify the calculations.

GENERAL ARRANGEMENT AND THEORETICAL PERFORMANCE OF THE WATERJET PROPULSOR

Among the available solutions for the Gluptak vehicle, a propulsion system composed of four waterjet propulsors seemed to be the most promising replacement for a screw propeller. However, low performance of the water jets was expected because of the vehicle's small dimensions and comparatively low speed. So, the proposal required detailed study regarding the geometry and operating parameters of the potential propulsor.

Description of the flow tunnel

The schematic outline of a waterjet propulsor is shown in the Fig. 6. It is composed of a flow tunnel and a pump rotor with a propulsion shaft. Characteristics of the flow tunnel are expressed with reference to points that are used to describe the waterjet. These are also measurement points and in accordance with the 23rd ITTC guidelines [8]. The flow tunnel elements are listed in Table 1 together with the semi-empirical formulas describing the flow losses due to the presence of these elements.

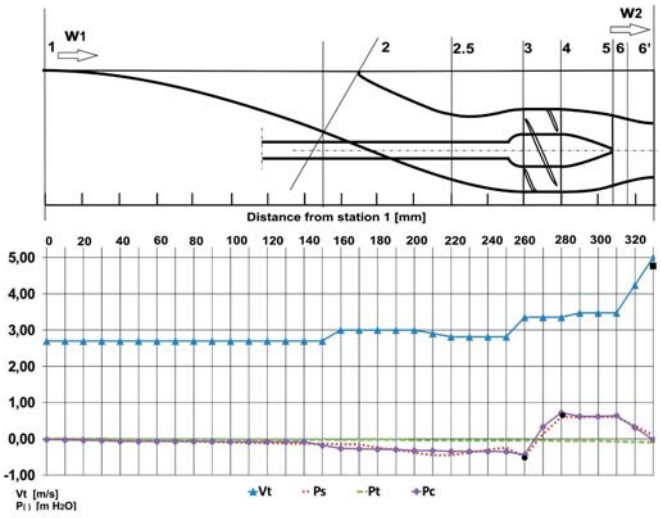

Fig. 6. The layout of the characteristic points (stations) and velocity symbols for station points of a waterjet propulsor following 23rd ITTC guidelines (top part) and results of study of flow inside the investigated 50 [mm] propulsor. Vt – flow velocity, Ps – total pressure calculated using CFD, Pt – pressure loss due to friction in the flow tunnel, and Pc – summary pressure estimated using semi-empirical models. Dots at 260 and 280 mm - pressures measured during experiment, square at 330 mm – measured output flow velocity

POWER AND EFFICIENCY OF A WATER JET PROPULSOR

Following Próchnicki [5], but without the assumption that the propulsor inflow velocity $\mathbf{w}_1$ is equal to the vehicle velocity **u**, the thrust force is generated by the jet stream ejected out of the outlet nozzle at station 6. It is a product of the mass flow rate and the difference of absolute velocities at the inlet and outlet of the propulsor.

$$F_u = m \cdot (c_2 - c_1) \tag{1}$$

The absolute inlet velocity c_1 is:

$$c_1 = w_1 - u \tag{2}$$

whereas the absolute outlet velocity c_2 is equal to the difference between the relative outlet velocity and vessel velocity:

$$c_2 = w_2 - u \tag{3}$$

Therefore, considering Eq. (2) and substituting Eq. (1) into Eq. (3) results in the thrust force of the working jet propulsor:

$$F_u = m \cdot (w_2 - w_1) \tag{4}$$

The greatest thrust force is generated for zero forward speed, which means high jet thrust force at the vehicle start.

$$F_u|_{u=0} = m \cdot w_2 = F_u max \tag{5}$$

The effective propulsion power is a product of the thrust force (equal to the vessel drag) and the vessel velocity:

$$N_u = F_u \cdot u = m \cdot (w_2 - w_1) \cdot u \tag{6}$$

The power of the outlet jet stream (carry-over loss) is described by the following equation:

$$N_{out} = m \cdot \frac{c_2^2}{2} = m \cdot \frac{(w_2 - u)^2}{2} \tag{7}$$

The pump power required to supply the propulsor is described by the power balance equation:

$$N_p \cdot \eta_p = N_u + N_{out} + N_{Loss} \tag{8}$$

So, calculation of the power required by the waterjet propulsor is easy to estimate if the tunnel losses and pump efficiency are known.

$$\eta_{WJ} = \frac{N_u \cdot \eta_p}{N_u + N_{out} + N_{Loss}} \tag{9}$$

The theoretical efficiency of a waterjet propulsor can be expressed by the formula below, which involves the velocity index μ:

$$\eta_{WJ}^{o} = \frac{2\cdot(1-\mu)\cdot\mu}{1-\mu^2+2\cdot\frac{N_{lo}}{m\cdot w_2^2}} = \frac{2\cdot(1-\mu)\cdot\mu}{1-\mu^2\cdot\left(1-2\cdot\frac{N_{lo}}{m\cdot u^2}\right)} \quad (10)$$

Where

$$\mu = \frac{u}{w_2} \quad (11)$$

is the non-dimensional velocity index.

A graphical representation of the relationships given by this formula is illustrated in the Fig. 7.

Considering the expression above, it can be seen that high efficiency is the result of the low carry-over loss, low tunnel loss, and high efficiency of the pump. It is apparent that, for the considered value of μ around 0.5, one can expect efficiency of between 50 and 60%, assuming moderate tunnel losses.

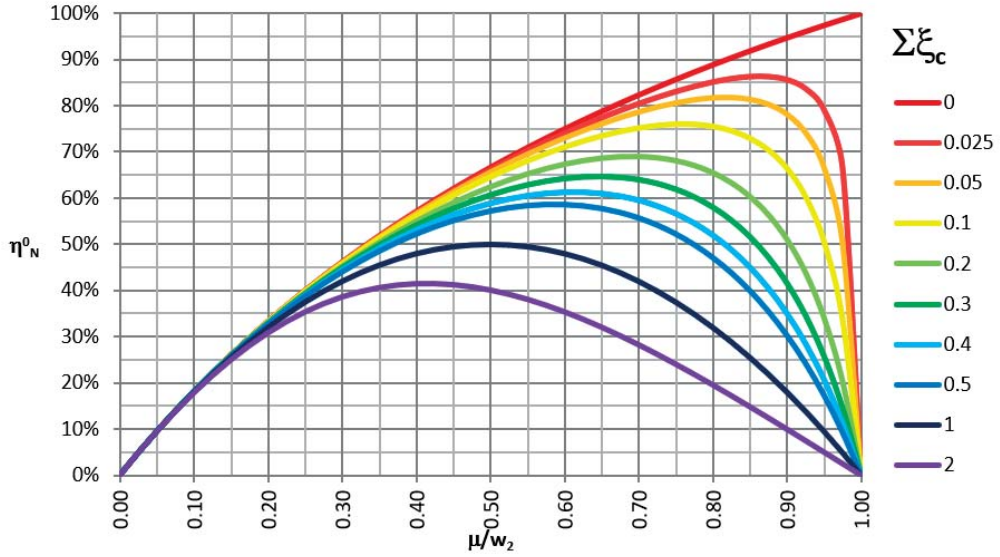

Fig. 7. Theoretical efficiency of waterjet propulsor

DESCRIPTION OF THE FLOW PARAMETERS USING BERNOULLI EQUATION

Following expression (9), the following values need to be estimated to calculate the efficiency of the waterjet propulsor:
- carry-over losses,
- flow losses inside the flow tunnel,
- efficiency of the pump.

The one-dimensional Bernoulli equation (12) was utilised to describe the flow parameters along the flow tunnel. It relates the velocities and pressures inside the flow tube if the usually used simplifying assumptions are valid:

$$\frac{\rho\cdot v^2}{2} + p = p_0 = constant \quad (12)$$

The graphical representation of the changes of the pressure and flow velocity along the flow tunnel, shown at the bottom of the Fig. 6, is a good tool to study the influence of local features on the tunnel flow behaviour.

The station points indicated on this figure make it possible to divide the waterjet propulsor into sections (elements). Each of these elements affects the summary flow losses in the propulsor duct at a different rate and their estimation is crucial for the design process. The elements refer to particular parts of the geometry of the propulsor.

SEMI-EMPIRICAL MODELS DESCRIBING THE TUNNEL LOSSES

Semi-empirical models describing the tunnel losses were assumed to be the best tool to investigate the influence of various propulsor parameters on its performance. These models use expressions proposed by several researchers who investigated particular phenomena in elements of flow duct. The performance of these tunnel elements is expressed by means of pressure (head) losses. Traditionally, pressure changes in the flow through pipes are expressed in [m] of water, which corresponds to the pressures generated by pumps expressed using the same units.

Particular expressions were selected for actual flow conditions, such as geometry ranges and the turbulence level expressed by the Reynolds number. They are listed in the Table 3, referenced to the tunnel elements.

The general equation describing flow energy (head) losses is Weisbach's formula [9]:

$$h_{l(i)} = \xi_{(i)} \cdot \frac{v^2}{2\cdot g} \quad (13)$$

The $\xi_{(i)}$ coefficient is the loss coefficient depending on the local geometry of the pipe element, such as the roughness, diameter reduction or expansion, pipe bend, protection grill etc.

Losses inside the flow tunnel were calculated separately for friction and local features. Therefore, the sum of flow losses expressed by the pressure drop in the fluid flowing through the tunnel is as follows:

$$h_l = \sum h_{fr} + \sum h_{ll} \quad (14)$$

As cavitation is not an issue for the considered application, there was no need to increase the pressure at the pump rotor space by means of increasing the rotor diameter relative to the flow pipe diameter. Therefore, for all calculations it was

assumed that the nominal diameter of the flow channel is equal to the diameter of the pump rotor. This also means that the nominal flow velocity inside the channel is equal to the velocity of the vehicle. The losses specific to the waterjet propulsor are commented upon below.

It was also assumed that the flow at the flow tunnel is fully developed and turbulent when the Reynolds number exceeds a value of 10^5. According to the available data, such a flow friction coefficient depends mainly on the surface roughness of a duct, as indicated on the graph developed by Holbrook and White and approximated by Altsul [1] in the form of expression (15):

$$\lambda = 0.11 \cdot \left(\frac{68}{R_e} + \frac{k}{d}\right)^{0.25} \tag{15}$$

where the k factor is surface roughness, assumed at 0.05 [mm] for all the considered cases. In practice, the roughness value cannot be scaled.

Velocity reduction between station 0 and station 1 – influence of the wake

The water that is ingested into the inlet of the waterjet tunnel partially originates from the hull's boundary layer. The mass-averaged velocity of the ingested water $\boldsymbol{v}_{in}$ is lower than the ship speed due to this boundary layer. The velocity deficit is expressed as the momentum wake fraction $\boldsymbol{w}$ and is defined as:

$$w = 1 - \frac{w_1}{u} \tag{16}$$

According to expression (4), the wake phenomenon increases the generated thrust but simultaneously, according to expression (6), increases the energy required to accelerate the water to the output velocity at station 6 to achieve the required thrust. Determination of the wake fraction is rather complex in the considered case, since the cross-sectional shape of the stream tube is not defined. Following Faltinsen, the

Tab. 1. The waterjet duct elements described using the station points

No.	Limiting stations	Element of the waterjet duct	Friction loss formula	Local loss formula
1	0 – 1a	Undisturbed flow far ahead of the vehicle	Not considered	Not considered
2	1a – 1	Area in front of the inlet influencing flow as turbulent boundary layer	reduction of average intake flow velocity	wake coefficient assumed $w = 1 - \frac{w_1}{u} = 0.05$
3	1	Local inlet loss due to start of the propulsor	–	wssumed at ξ_{lin} =0.05
4	1 – 2	The inlet semi-open pipe, bend	ξ_{fin} = (λ(l/d))/2	$\xi_{fin} = \left[0.131 + 0.163 \cdot \left(\frac{d}{R_{in}}\right)^{3.5}\right] \cdot \frac{\gamma_{in}}{90}$
5	2	The pipe inlet	–	assumed at ξ_{fp} =0.2
6	2 – 3	The pipe, the pipe bend	ξ_{fpi} = λ(l/d)	$\xi_{fpb} = \left[0.131 + 0.163 \cdot \left(\frac{d}{R_{pb}}\right)^{3.5}\right] \cdot \frac{\gamma_{pb}}{90}$
7	3 – 4	The diffuser	$\xi_{fd} = \frac{\lambda_t}{8\,sin\left(\frac{\delta_D}{2}\right)} \cdot \left[\left(\frac{A_{D2}}{A_{D1}}\right)^2 - 1\right]$	$\xi_{ld} = k_p \cdot \left(\frac{A_2}{A_1} - 1\right)^2$ k_p= 0.14,
8	3 – 5	The pump pipe	ξ_{pp} = λ(l/d)	–
9	5	The inlet to the pump stator due to introduction of the stator blades	–	assumed $\xi_{ls} = 0.1$
10	4 – 5	The pump stator	$\xi_{fS} = \frac{2 \cdot \lambda_t}{8\,sin\left(\frac{\delta_C}{2}\right)} \cdot \left[1 - \left(\frac{A_{S2}}{A_{S1}}\right)^2\right]$	$\xi_{lS} = 0.04 + \left(\frac{1}{\chi} - 1\right)^2$ χ=0.9
11	5 – 6	The nozzle	$\xi_{fN} = \frac{2 \cdot \lambda_t}{8\,sin\left(\frac{\delta_N}{2}\right)} \cdot \left[1 - \left(\frac{A_{N2}}{A_{N1}}\right)^2\right]$	$\xi_{lN} = 0.04 + \left(\frac{1}{\chi} - 1\right)^2$ χ =0.9

wake fraction "may vary between 0 and 0.4 for a displacement vessel, depending on the hull form" [10].

The thickness of the turbulent boundary layer develops from the beginning of the vehicle body following changes of the value of the Reynolds number along the flow, where $\boldsymbol{x}$ is the distance from the beginning of the body.

$$Re_x = \frac{v \cdot x}{\nu} \tag{17}$$

For a flat plate, the flow is laminar up to $R_e < 0.2 \cdot 10^6$ and completely turbulent above $R_e > 3 \cdot 10^6$. However, because of the spherical nose, substantial turbulence may develop at the beginning of the spherical body. It is further amplified by several local obstructions present on the body of the vehicle.

Standard theory for a flat plate boundary layer, as described in several textbooks [10] [11], [12] can be used to get a first indication of the velocity distribution. It is convenient to use a power-law velocity profile for the thickness of the boundary layer [10]:

$$\delta = \frac{0.16 \cdot x}{(Re_x)^{1/7}} \tag{18}$$

According to expression (18), the thickness of the turbulent layer develops as shown in the Fig. 8. Fully developed turbulent flow is initiated just at the propulsor's inlet, and its thickness is about 25 [mm]. This value corresponds well with data obtained from CFD simulations in the flow.

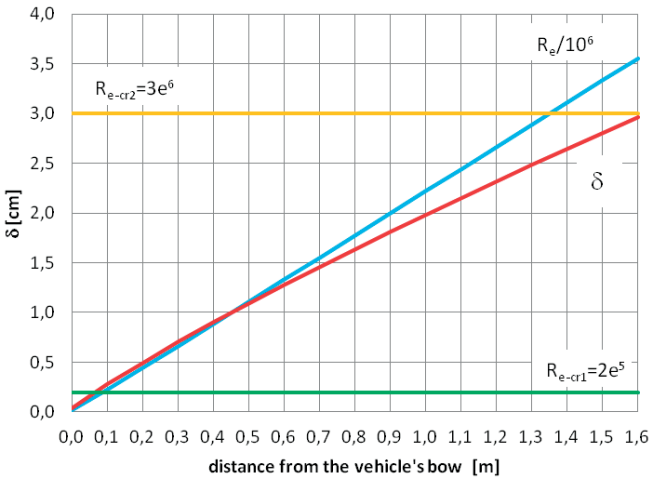

Fig. 8. Thickness of the boundary layer along a flat plate at water temperature of 15 [°C]

The CFD calculations, performed in parallel to this study, have indicated the average stream tube flow velocity as 2.7 [m/s] at station 1 of the propulsor, which corresponds to w = 0.1. However, the intermediate value of w=0.05 was adopted for the performance analyses because the assumed flow tube height is twice the thickness of the boundary layer. One needs to be aware of the substantial influence of the value of the wake friction coefficient on total propulsor performance. If w = 0.1 were assumed, the total water jet efficiency estimated would rise by 5% for a 50 [mm] rotor diameter. Contrarily, for w = 0.0 the efficiency value would drop by 5%.

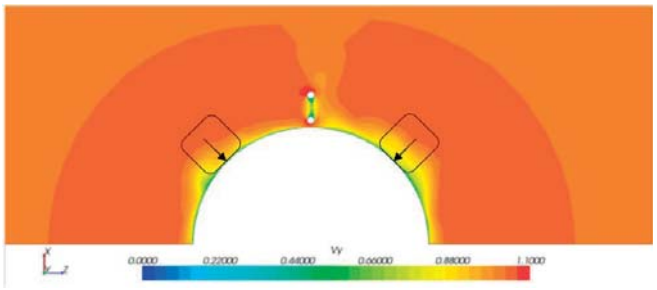

Fig. 9. Distribution of flow longitudinal relative velocities at the plane coincident with station 1 of waterjet propulsors. Reference velocity is 3 [m/s]. Flow intakes are indicated by arrows, stream tubes are indicated by rounded squares.

Tunnel inlet

Usually, the tunnel inlet of a water jet is a rectangular or oval opening in the vehicle hull. The 21st ITTC [13] recommends intake proportions at a ratio of 1.3:1.0 (length about 30% greater than width), but other research [8] indicates that changes within 20% in the proportions of the capture area deliver only about 1% difference in the estimated power (thrust). Moreover, van Terwisga [14] concluded that there was no significant effect on power (thrust) losses or gains between rectangular and elliptical intake shapes. He also found that variations of thrust are contained within 0.5% for the inlet proportions 1.3:1 and 1.5:1 (length: width). Also CFD analysis of the inlet with a trapezoidal shape suggests that there is no necessity to determine the inlet area precisely. Other researchers [6], [10], [15], indicate that this area is as important as the rest of the flow duct and cannot be neglected. It determines the character of the inflow to the next stage and has a substantial influence on drive efficiency. Therefore, it is recommended to analyse it precisely and perform further scrutiny of this area [8]. For the initial phase of investigation, the local loss coefficient of a constant value was assumed and it was later studied with the CFD method.

Tunnel bend at the inlet

The *Coandă effect* [16] is the tendency of a fluid flow to be attracted to a nearby surface. In practice, the *Coandă effect* changes the direction of the flow. If the surface curvature is smooth enough, it causes the fluid to stick to it. Fluid follows the surface until it ends sharply or the fluid stream is faced with some obstacle. In a case of the waterjet propulsor, the effect can be observed at the tunnel inlet where a part of the stream flowing around the vehicle's body is redirected to the duct. The obvious advantage of this phenomenon is that, at least partially, it fills the inlet space with water. This in turn reduces the amount of water that needs to be sucked in and thus increases the overall performance of the propulsor.

Unfortunately, the precise determination of the water stream flowing into the tunnel is very difficult due to the nature of this natural phenomenon. Hence, the losses

estimations at this stage are only anticipations based on formulas related to a sudden change of flow direction or bend of a pipe.

THE PUMP AS ELEMENT OF THE WATERJET PROPULSOR

The pump efficiency of a waterjet propulsor is the second basic parameter, beside channel losses, that needs to be estimated to obtain its (WJ) overall efficiency. The pump rotor-stator part of the waterjet propulsor can be regarded as a standard pump section. The most popular types of pumps used in waterjet drives are axial, diagonal (mixed-flow), and helicoidal pumps (in outboard motors). There is limited information regarding the design of pumps of the considered parameters: rotor diameter D < 0.050 [m], head (output pressure) H< 2 [m] and volumetric output q < 10 dm^3/s] ~(Q < 20 [m^3/h]). In particular, there are no data regarding these parameters for axial pumps. So, general rules regarding assessment of the pump performance need to be applied in the case considered. An axial type pump was assumed for the propulsor. The choice was supported by general selection rules based on the pump kinematic speed index $\mathbf{n}_{SQ}$, the value of which is defined by formula (11). It depends on the relation between $\boldsymbol{Q}$, $\boldsymbol{H}$ and $\boldsymbol{n}$, and it is closely related to the pump geometry. The speed index allows for comparison of pumps with identical dynamic characteristics but different geometry, and selection of the most appropriate type.

$$n_{sQ} = \frac{n \cdot Q^{1/2}}{H^{3/4}} \tag{19}$$

For the assumed parameters, its value is around 300 as most suitable for axial type pumps. Most sources present pump characteristics in the form of charts. There are some general data regarding performance and general rules regarding the selection of rotary pumps. The two graphs in the Fig. 10 show the efficiency of a wide range of pumps referenced to the pump velocity index. The diagram in the Fig. 10(a) suggests the application of an axial pump in the case considered. Axial pumps with a volumetric capacity of ~20 [m^3/h] are considered very small and are rarely optimised to reach high efficiency. However, there is still a possibility to compare pumps of different sizes and hence obtain essential input data for semi-empirical calculations. According to both graphs in the Fig. 10, the pump efficiency for a pump with the assumed volumetric flow and a speed index of 300 has a value between 60% and 65%.

Some authors propose simple formulas that are supposed to determine the total performance of a pump, based on the model (reference) pump efficiency. Selected ones are listed in the Table 2, where the $\boldsymbol{m}$ index refers to the model pump. The $\boldsymbol{d}$ and $\boldsymbol{d}_m$ are pump rotor and the pump model rotor (reference) diameters respectively. These (21), (23), usually require some data regarding the speed of both pumps. In the case of a lack of information regarding the speed of the reference pump, the much simpler formula (22), developed by H.H. Anderson, can be used. For the purpose of this work, it was assumed that the reference pump had a 0.5 [m] rotor diameter and 90% efficiency at the operating point. These values are typical for large waterjet pumps [17]. Hence, for a rotor with 0.05 [m] diameter and using the *Anderson's* formula, the calculated efficiency is over 82%. It drops to just below 80% for a 30 [mm] diameter pump rotor. For further consideration, less optimistic efficiencies based on expression (23) and the data listed in the Table 2 were assumed.

According to these data, for a pump with a considered volumetric flow of ~20 [m^3/h] (0.005 [m^3/s]) and speed index of 300, the efficiency value would be estimated below 65%. To be on the safe side, the value of 60% was assumed for a rotor diameter of 50 [mm]. The efficiency values used for various investigated diameters are presented in the Table 3.

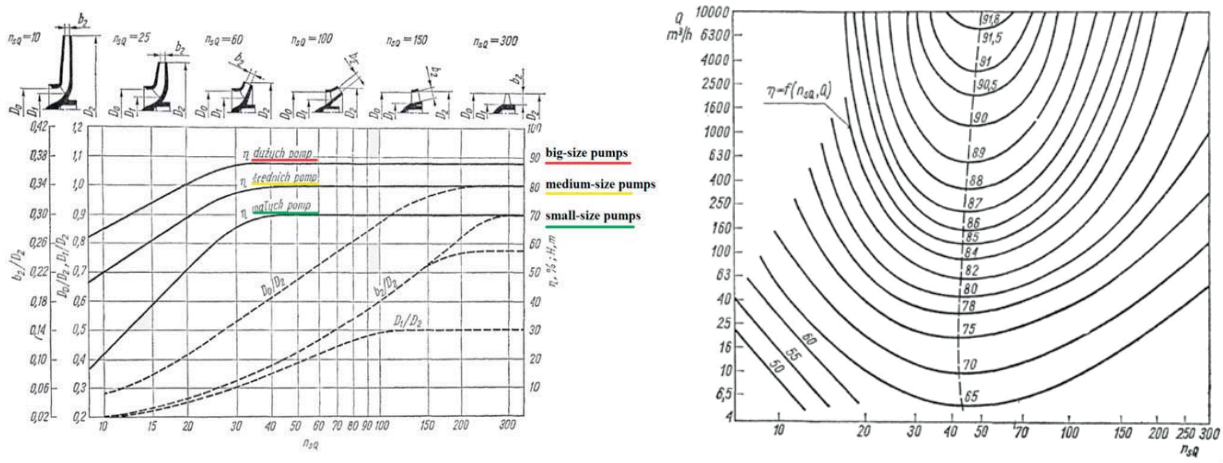

Fig. 10. General performance curves and selection rules of a rotary pump based on pump kinematic speed index by Neumaier and Gradewald in [12]

Tab. 2. Expected efficiencies of an axial pump for a low diameter waterjet propulsor

No.	Source of data	Formula	Efficiency
1	Gradewald [12]	Diagram in Fig. 10(a)	~ 60%
2	Neumaier [12]	Diagram in Fig. 10(b)	< 70%
3	Moody's formula [18]	$\eta = 1 - (1 - \eta_m) \cdot \left(\frac{d_m}{d}\right)^{0.45} \cdot \left(\frac{n_m}{n}\right)^{0.2}$ (21)	68% for d=0.05 m
4	Anderson [9], [19]	$\eta = 1 - (1 - \eta_m) \cdot \left(\frac{d_m}{d}\right)^{0.25}$ (22)	82% for d=0.05 m
5	Arnold & Nijhuis [17]	$\eta = 0.95 - \frac{0.05}{\sqrt[3]{\frac{Q}{Qm}}} - 0.125[log(n_\omega)]^2$ (23)	65% for d=0.05m Q=0.006 m³/s $n_\omega = 3$
6	Kim & Chun [2]	Experimental results for 64 mm rotor diameter 0.7% blade tip clearance 1.5 % blade tip clearance	61% 54%

Tab. 3. Efficiencies of axial pumps of small size waterjet propulsors depending on the rotor diameter assumed for semi-empirical calculations

No.	Parameter	Unit	Value				
1	Pump rotor diameter	[mm]	30	40	50	60	70
2	Estimated pump efficiency	[%]	50	57	60	62	64

EVALUATION OF BASIC PARAMETERS OF THE WATERJET PROPULSOR FOR ASSUMED OPERATIONAL CONDITIONS

Geometric limitations are important factors while considering the replacement for open screw propellers by means of waterjet propulsors. To preserve the propulsion and manoeuvring capabilities of the existing vehicle, it was assumed that the propulsion system needs to be arranged using the existing configuration. This assumption indicated a solution with the four units arranged in an X configuration. To minimise drag resistance, the waterjet propulsors were built into the stabilising fins to ensure undisturbed flow around the fins and external surfaces of the propulsors. The pump rotor diameter is to be possibly small for the same reason. The initial diameter of the pump rotor of the waterjet propulsor can be calculated using the following expression:

$$D_{opt} = 1.45\sqrt[4]{\frac{F}{\rho n^2}} \quad \textbf{(20)}$$

It is further advised to adopt the diameter evaluated using this expression or the largest diameter allowed by the geometry of the vehicle. In the case considered, it was found (Fig. 11) that the rotor diameter is to be around 50 [mm] if a rotational speed near 5000 [rpm] is assumed.

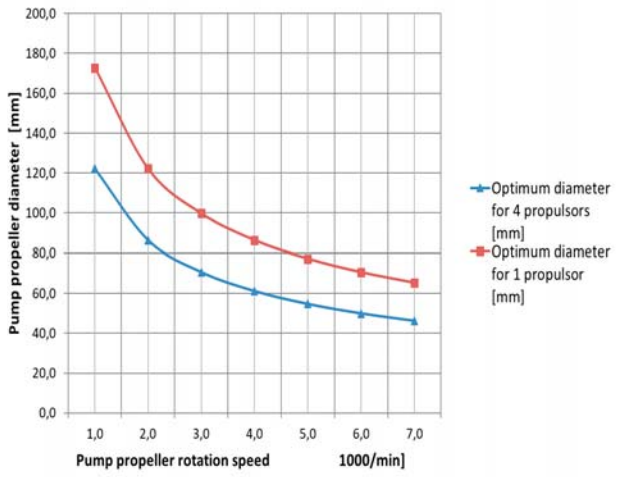

Fig. 11. Optimum pump rotor diameter calculated using expression (20) for the vehicle propelled by a single water jet propulsor with 56 [N] of thrust and or four water jet propulsors with 14 [N] of thrust

While the pump rotor diameter lower than 50 [mm] was found to be possibly appropriate in the considered application, a range of pump rotor diameters of 30, 40, 50, 60 and 70 [mm] was defined for further evaluation. Additional assumptions for comparison of the waterjet propulsors with the nominal diameters listed above were as follows:

1. The nominal flow velocity inside the pipe component of the propulsor is equal to the nominal velocity of the vehicle (v_{pipe}=u=3 [m/s]);
2. The nominal diameter of a flow channel (pipe) between station 2 and station 2.5 was assumed to be equal to the nominal propeller diameter.

The following calculation algorithm was executed to find the rotor diameter that ensures the required thrust and highest possible efficiency:

1. The nozzle output flow velocity $\mathbf{w}_2$ was set at a value that ensures the required thrust of 14 [N];

2. The fluid velocity at every tunnel component was calculated, using data regarding the geometry of this tunnel component;
3. The coefficient of losses for every component was calculated, split into friction $\xi_{f(i)}$ and local losses $\xi_{l(i)}$;
4. The pressure losses of all the components (friction and local) were summed along the tunnel, starting from station 1;
5. The pressure change due to change of water velocity at a point or a tunnel element was calculated;
6. All pressure changes including that resulting from the operating rotor were summed up along the tunnel, starting from station 1;
7. The power required to compensate the corresponding drop of pressure carry-over losses and ship propulsion was calculated;
8. The pump head was calculated for the propulsion power required.

Friction losses in a considered element of the tunnel were calculated for the end of this element. Local losses were introduced at the station where they occurred (input 1 at station 1, input 1 at station 2, and input to pump stator) or for the end of a local feature (bend, diffuser, pump stator, confusor).

CALCULATION RESULTS

Excel spreadsheets were used for calculations using the semi-empirical algorithm. The resultant values for a water temperature of 15 [°C] are summarised in the Table 4. It contains the basic parameters of the flow parameters for characteristic points and elements of the flow tunnel. The calculated results describe averaged parameters of the flow in great detail and allow for study of the influence of a particular element of the geometry of the flow tunnel on the final performance of the propulsor. Fig. 6 shows these results for the 50 [mm] nominal rotor diameter in graphical form. The figure refers to the tunnel itself. For graphical presentation purposes, the values of friction losses between stations were linearly approximated. Local losses were introduced at the station of occurrence (pipe inlet loss, stator input loss) or linearly approximated between stations (bends, diffuser, confuser). Changes of flow velocities were introduced at the end of an element and linearly approximated between stations.

Tab. 4. Comparison of the relative parameters of waterjet propulsors with various pump rotor diameters for assumed thrust of 14 [N] and wake coefficient w=0.05

No.	Parameter	Symbol	Unit	Pump rotor diameter [mm]				
				30	40	50	60	70
1	Velocity of the vehicle	$\mathbf{u}$	m/s	3.00	3.00	3.00	3.00	3.00
2	Velocity at station no. 6	$\mathbf{w_2}$	m/s	9.45	6.56	5.23	4.50	4.06
3	Velocity index	$\mu=\mathbf{u}/\mathbf{w_2}$	-	0.32	0.46	0.57	0.67	0.74
4	Water jet thrust	F_u	N	14	14	14	14	14
5	Sum of coefficients of losses	$\Sigma\xi_c=\Sigma\xi_f+\Sigma\xi_l$	-	0.726	0.640	0.595	0.572	0.563
6	Pump output power required	N_p	W	95	78	72	71	75
7	Theoretical total waterjet efficiency	η_{wj0}	%	43	52	55	54	49
8	Estimated total waterjet tunnel efficiency	η	%	44	53	56	56	53
9	Estimated pump efficiency	η_p	%	55	57	59	60	61
10	Calculated pump speed index (kinematic)	Nsq	-	99	181	269	353	469
11	Estimated total propulsor efficiency	η_{prop}	%	22	30	34	35	34

Tab. 5. Energy (power) distribution in waterjet propulsors with pump rotors of different diameters

No.	Parameter	Symbol	Unit	Pump rotor diameter [mm]				
				30	40	50	60	70
1	Estimated motor output power required	N_m	W	191	138	124	121	124
2	Vehicle propulsion power	N_u	W	42	42	42	42	42
3	Relative propulsion power (= total water jet efficiency η_{prop})	ψ_u	%	22	30	34	35	34
4	Pump relative loss	Ψ_p	%	50	43	40	38	40
5	Carry-over relative loss	ψ_{co}	%	23	17	12	8	5
6	Sum of tunnel-related relative losses	Ψ_t	%	4	8	14	19	23
7	Tunnel friction relative losses	Ψ_f	%	2	3	4	5	5
8	Inlet (before pump) relative losses	ψ_{in}	%	1	3	6	9	12
9	Outlet (after pump: pump stator and confuser) relative losses	ψ_{out}	%	1	2	4	5	6

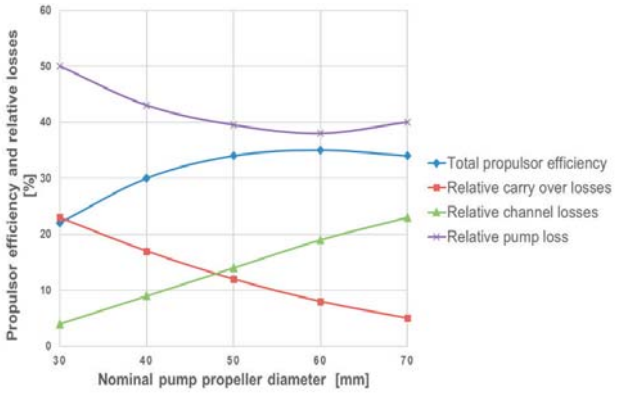

Fig. 12. Development of power distribution in small water jet propulsor depending on the pump propeller diameter (total propulsion efficiency = relative propulsion power).

CFD CALCULATIONS AND REAL EXPERIMENTS

For the selected nominal diameters of the propulsors (rotors), 3D geometrical models were prepared and studied using CFD flow calculations. The results of one of the simulations regarding a 50 [mm] nominal diameter are shown in the Fig. 6 in the form of the curve representing pressure changes in the flow duct.

As can be seen, there is good coincidence of the results of the semi-empirical and CFD calculations. The semi-empirical algorithm offers quite good modelling of the real performance of the whole waterjet propulsor that allows for rapid assessment of the principal geometric parameters. However, the numerical calculations offer the opportunity to study local phenomena of the flow in great detail. In fact, several detailed studies were performed to find the influence of the local geometries of the flow tunnel performance. Beginning from the inlet (station 1), the following issues were investigated:

1. Raising the inlet point above the hull surface to avoid intake of the turbulent layer.
2. Flash inlet geometry.
3. Curvature radius of the tunnel bent between station 1 and station 2.
4. Curvature radius of the tunnel bent between station 2 and station 3.
5. P/D ratio of pump rotor blades.
6. Geometry of the stator and stator blades between station 4 and station 5.
7. Geometry of the nozzle between stations 5 and 6.

The results of the CFD calculations of particular features as well as the results of tests of real propulsors will be presented in a separate publication.

SUMMARY

1. The results of the study confirm the usefulness of the semi-empirical method in the evaluation of the basic parameters of the waterjet pump rotor of unusual size.
2. The influence of the shape of the local cross-section area of the tunnel on the local flow parameters cannot be studied using the semi-empirical method.
3. Detailed design of local features requires the application of CFD methods, which proved to give realistic results.
4. A propulsor with a nominal diameter of 50 [mm] was selected for further investigations as offering the best compromise between its performance and low influence on the vehicle drag.
5. In practical terms, the study justifies the replacement of open screw propellers with water jets without a substantial penalty on the Gluptak vehicle's propulsion performance. This is true in spite of the much lower efficiency of the waterjet propulsor because of the possibility of removal of the fibre protection grill. The calculated motor output power of 124 [W] exceeds the assumed value of 120 [W] by just 3%.
6. Other issues regarding the underwater vehicle's performance such as its directional stability and the ability to manoeuvre require separate studies as well as solutions, and may influence the final propulsor configuration.

NOMENCLATURE

ρ – water density [kg/m^3]
g – gravity acceleration [m/s^2]
u – ship speed [m/s]
w – wake factor [-]
w_1 – water velocity of inflow to flow channel [m/s]
w_2 – outflow from confusor [m/s]
μ – velocity index [–]
$v_{(i)}$ – flow velocity, general [m/s]
ν – fluid viscosity [m^2/s]
D – nominal diameter of propulsor (flow channel and pump rotor) [m]
D_N – diameter of outlet nozzle [m]
D_m – nominal diameter of reference (model) pump [m]
$d_{(i)}$ – local diameter of the flow channel [m]
δ_D, δ_S, δ_N, – diffusor, stator and nozzle divergence angle [deg]
F_u – thrust force [N]
m – rate of water mass flow through propeller [kg/s]
Q – volumetric output [dm^3/s]
P_r – pitch of pump rotor [m]
k – surface roughness [mm]
λ – pipe friction coefficient [-]
$\boldsymbol{\zeta_{f(i)}}$, $\boldsymbol{\zeta_{l(i)}}$ – dimensionless coefficient of hydraulic losses due to friction and local channel geometry.
H, p – pressure in flow duct [m H_2O]]
H_p – pump head (output pressure) [m H_2O]
$h_{lo(i)}$ – local pressure or pressure loss [m H_2O]
$\boldsymbol{N_u}$ – vehicle propulsion power [W]
$\boldsymbol{N_{co}}$ – power to carry-over losses [W]

N_{lo} – power of losses [W]
N_m – estimated motor output power required [W]
η_{wj0} – theoretical total waterjet efficiency [%]
η_p – pump efficiency [%]
η_m – specific efficiency [%]
$\psi_{(i)}$ – relative losses inside an element of the flow channel or due to local flow phenomenon [%]
R_{in}, R_{pb} – radius of flow channel bent at intake and pipe [m]
n – pump rotor rotation speed [1/s]
n_{SQ} – pump velocity index (Q[m³/s], n [rpm], H[m])
n_ω – pump velocity index (Q[m³/s], n [rad/s], H[m])

REFERENCES

1. Y. Shen *et al.*, 'Design of Novel Shaftless Pump-Jet Propulsor for Multi-Purpose Long-Range and High-Speed Autonomous Underwater Vehicle', *IEEE Trans. Magn.*, vol. 52, no. 7, 2016, doi: 10.1109/TMAG.2016.2522822.
2. L. Zhang, J. N. Zhang, Y. C. Shang, G. X. Dong, and W. M. Chen, 'A Practical approach to the assessment of waterjet propulsion performance: The case of a waterjet-propelled trimaran', *Polish Marit. Res.*, vol. 26, no. 4, 2020, doi: 10.2478/pomr-2019-0063.
3. L. Jian, L. Xiwen, Z. Zuti, L. Xiaohui, and Z. Yuquan, 'Numerical investigation into effects on momentum thrust by nozzle's geometric parameters in water jet propulsion system of autonomous underwater vehicles', *Ocean Eng.*, vol. 123, 2016, doi: 10.1016/j.oceaneng.2016.07.041.
4. S. Wang, M. Fu, Y. Wang, and L. Zhao, 'A Multi-Layered Potential Field Method for Water-Jet Propelled Unmanned Surface Vehicle Local Path Planning with Minimum Energy Consumption', *Polish Marit. Res.*, vol. 26, no. 1, 2019, doi: 10.2478/pomr-2019-0015.
5. W. Próchnicki, *Analysis of the ship's jet propulsion capabilities*. Gdansk: Politechnika Gdanska, 2001.
6. L. Rowinski, 'Motion requirements of single mission mine counter submersible craft, Underwater Defence Technology Conference and Exhibition, Malmo, Sweden', 2003.
7. L. Rowinski, 'Articulated warhead mine disposal vehicle, Underwater Defence Technology Conference and Exhibition "UDT Europe 2008", Glasgow, Great Britain', 2008.
8. 'The Specialist Committee on Validation of Waterjet Test Procedures', in *Proceedings of the 24th ITTC*, 2005, p. Volume II.
9. F. M. White, 'Fluid Mechanics seventh edition by Frank M. White', *Power*, 2011.
10. F. O. M. Faltinsen, *Hydrodynamics of High-Speed Maritime Vehicles*. Cambridge University Press, 2005.
11. Tesch Krzysztof, *Fluid Mechanics*. Politechnika Gdanska, 2008.
12. H. T. Schlichting, *Boundary Layer Theory*. McGraw-Hill, 1979.
13. 'Report of the Waterjets Group, Proceedings of the 21st International Towing Tank Conference, ITTC'96', Trondheim, Norway, 1996.
14. T. J. C. Van Terwisga, 'Waterjet-Hull interaction, PhD. Thesis', 1996.
15. M. C. Kim and H. H. Chun, 'Experimental Investigation into the performance of the Axial-Flow-Type Waterjet according to the Variation of Impeller Tip Clearance', *Ocean Eng.*, vol. 34, no. 2, 2007, doi: 10.1016/j.oceaneng.2005.12.011.
16. C. Lubert, 'On some recent applications of the coanda effect', in *International Journal of Acoustics and Vibrations*, 2011, vol. 16, no. 3, doi: 10.20855/ijav.2011.16.3286.
17. J. Arnold; G.J. Nijhuis, *Selection design and operation of rotodynamic pumps. The Nijhuis Pompen*. 2005.
18. L. F. Moody, 'The Propeller Type Turbine', *Trans. Am. Soc. Civ. Eng.*, 1925.
19. H. H. Anderson, 'Theory of Centrifugal Pumps', in *Centrifugal Pumps*, 1993, pp. 36–43.

CONTACT WITH THE AUTHORS

Lech Rowinski
e-mail: rowinski@pg.edu.pl

Gdańsk University of Technology
Narutowicza 11/12, 80-233 Gdansk,
Poland